Single Molecule Visualization of Stable, Stiffness-Tunable, Flow-Conforming Worm Micelles

Paul Dalhaimer,[†] Frank S. Bates,[‡] and Dennis E. Discher*[,†]

Department of Chemical and Molecular Engineering, University of Pennsylvania, Philadelphia, Pennsylvania 19104-6391, and Department of Chemical Engineering and Materials Science, University of Minnesota, Minneapolis, Minnesota 55455

Received January 29, 2003; Revised Manuscript Received July 2, 2003

ABSTRACT: We describe fluorescence visualization of highly stable worm micelle superpolymers. The worm micelles are self-assembled in water from nonionic, block copolymer amphiphiles. By blending and polymerizing inert and cross-linkable copolymers, we form micelles up to tens of microns long with persistence lengths that continuously span more than 2 orders of magnitude from submicron to submillimeter. In flow, pristine worms orient and stretch with DNA-like scaling, and their stability, loading capacity, and stealthiness make them ideal candidates for flow-intensive delivery applications such as phage-mimetic drug carriers and micropore delivery.

Introduction

Worm micelles are amphiphilic aggregates poised between molecular scale spherical micelles and much larger lamellar structures such as vesicles. Assembly of diblock copolymer amphiphiles into one of these microstructures depends primarily on the weight fraction, *w*, of the hydrophilic block relative to the total copolymer molecular weight.[1−3] For poly(ethylene oxide) (PEO)-based diblocks in aqueous solution, $w_{EO} \approx 45-55\%$ leads to the assembly of mainly worm micelles (Figure 1a).[4,6] Higher *w* gives predominantly spherical micelles, and lower *w* yields vesicles.[5] Despite this sensitivity in composition, the worm micelle assemblies here of 4000−5000 g/mol diblocks prove exceedingly stable yet flexible. Once formed, worms in aqueous solution are labeled by adding a hydrophobic fluorescent dye, which allows for visualization. The dye incorporates into the hydrophobic cores of the worms in a matter of seconds.

The fluorescence microscopy sequence in Figure 1b shows a labeled, highly stable worm extending in flow among obstacles (I)—in this case blood cells. The worm then expands (II) and sequesters in a stagnant zone (III). While illustrative of the stability, flexibility, and convective response of worms, such results are also suggestive of micro- or nanoapplications in micellar drug delivery and pore chemistry where flow is highly directing. Vesicles and spherical micelles have already been widely studied in such applications; worms are an intermediate microphase, which motivates a deeper understanding of their dynamics. Using two worm-forming diblocks (structural details in Table 1)—one with an inert hydrophobic block of PEE (polyethylethylene), designated OE6, and another with cross-linkable PBD (polybutadiene), designated OB3—we elucidate the control one has over worm shape and flexibility. We also highlight the stability imparted by such block copolymer amphiphiles whose molecular weight, *M*, is 5−10 times that of typical lipids.[4,6]

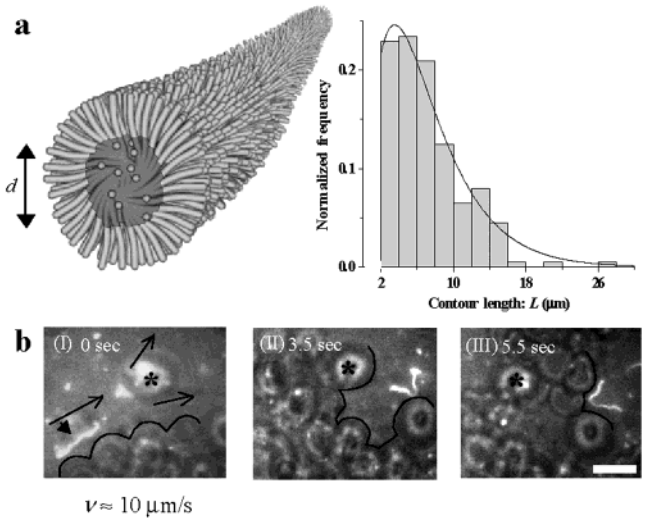

Figure 1. Wormlike micelles formed from the diblock copolymers PEO−PEE and PEO−PBD. (a) Schematic illustration of a worm with $d \approx 14$ nm core.[4] Spheres represent dye molecules. The inset distribution of measurable contour lengths, *L*, is fit by $Freq = L \exp(-L/L^*)$, where $L^* = \sqrt{(C e^{\alpha})}$ with $C \sim 1$ mg of copolymer/mL of H_2O at worm formation and α as the energy driving self-assembly.[5] (b) Snapshots of a pristine worm in a suspension of blood cells. For several seconds, the worm is elongated by a flow of $v \approx 10$ μm/s (I) before being sequestered in a stagnant zone where the worm simply diffuses (II and III). Worms clearly do not stick to the cells. The reference cell (∗) is stuck to the coverslip. Scale bar is 10 μm.

Table 1. Structural Details of Poly(ethylene oxide)−Polybutadiene (OB) and Poly(ethylene oxide)−Polyethylethylene (OE) Diblock Copolymers

designated name	polymer formula	M_n (kg/mol)	w_{EO}	*d* (nm)
OB3	$EO_{55}-BD_{45}$	4.9	0.51	14.2[4]
OE6	$EO_{46}-EE_{37}$	4.1	0.48	12.5[5]

Fluorescence video microscopy has, of course, been applied to study the dynamics of DNA,[8] microtubules,[9] and F-actin,[9,10] but these biopolymers are complex polyelectrolytes.[8,9] Solution ionic strength, multivalent ions such as Ca^{2+},[11] metabolic substrates (like ATP),[12] contaminating cross-linker proteins, and oxidation[11] (e.g., disulfide cross-links) are all among the most

[†] University of Pennsylvania.
[‡] University of Minnesota.
* To whom correspondence should be addressed: e-mail dischar@seas.upenn.edu.

10.1021/ma034120d CCC: $25.00
Published on Web 08/13/2003

compounding of factors, and all of these can profoundly influence polymer dynamics, aggregation states, and collective rheology. The viscoelasticity of F-actin, for example, continues to be enigmatic and plagued by preparation effects.[13] The PEO−PEE and PEO−PBD worm systems here have a simpler composition of strongly segregating, nonionic copolymers with just two monomer types (three when blended) plus dye as opposed to 19 amino acids in proteins or four base pairs in a complex DNA sequence, plus counterions, dyes, etc. The worms here—formed by stirred hydration of a dried block copolymer film—also have a brushy PEO corona that tends to sterically stabilize these worms and minimize interactions with other worms and surfaces (e.g. Figure 1b). These stable, superpolymer aggregates would seem ideal for addressing dynamical questions concerning polymeric objects, such as internal vs external viscosity effects[14] and collective rheology of synthetic[15] and biological[16] systems. They also establish a foundation for focused material applications.

Experimental Section

Materials. The copolymers listed in Table 1 were synthesized using anionic polymerization techniques described elsewhere.[17] The number of monomer units in each block was determined from ^{1}H NMR. The molecular weights of the copolymers were determined using gel permeation chromatography with polystyrene standards.

Preparation of Worm Micelles. Worm micelles were formed in water at 55−60 °C using film hydration techniques.[18] Worms were then labeled with a hydrophobic fluorescent dye (PKH26; Sigma) in a molar ratio of 1:3 dye:copolymer. The dye was added directly to the aqueous solution of worms.

Fluorescence Microscopy. The backbone contours of the worms were visualized with a Nikon TE-300 inverted fluorescence microscope (TRITC; Chroma). The worms were confined between a coverslip and a slide which were spaced ∼1 μm apart using polystyrene beads as spacers. Video-rate images of the worms were collected with an ICCD camera (Princeton Instruments).

Results and Discussion

Stability and Flexibility. Because of the kinetic barrier to further aggregation and the strong association of the large hydrophobic blocks, worms tend to be stable assemblies as indicated by the contour length distribution (Figure 1, inset) which persists for at least a month. Fits of such a distribution yield a minimum self-association energy $\alpha \approx 26k_BT$, which is indeed far higher than the $\alpha \approx 10k_BT$ typical of small amphiphile assemblies.[5]

For pristine worms of OB3 or OE6, sequential snapshots and overlays of skeletonized contours demonstrate the considerable flexibility of this fluid system (Figure 2a). An autocorrelation time for relative end-to-end length (R/L) of $\tau_{R/L} = 2.6 \pm 0.6$ s allows for accurate visualization as well as adequate statistical measures, where distances are measured from fluorescence video images. A self-avoiding chain fluctuating in d^*-dimensions is expected to increase in size as $\langle R\rangle = a^{1-\theta}L^{\theta}$, where a is the blob size in a bead-on-string model and the scaling exponent $\theta = 3/(2 + d^*)$.[19] Since the worms here are confined to a ∼1 μm gap defining a pseudo-two-dimensional geometry, we expect $\theta \approx {}^3/_4$ and find $\theta = 0.84 \pm 0.06$. This is in close agreement with $\theta = 0.79 \pm 0.04$ found previously for DNA adsorbed to a cationic lipid membrane.[8]

The persistence length of the un-cross-linked worms is $l_P = 500 \pm 200$ nm, estimated from the relation $\langle R^2\rangle = 2l_P^2[L/l_P - 1 + \exp(-L/l_P)]$, where l_P is divided by two since the worms are confined to a pseudo-2D gap.[20,21] This proves to be the same as l_P (=570 nm) obtained from small-angle neutron scattering data fit to the Kratky−Porod model,[19] and implies that dye labeling is minimally perturbing.

The persistence length of a self-assembled worm proves useful to understanding the molecular basis for its rigidity, noting that $l_P = \kappa/k_BT$, where κ is the bending rigidity. A D-dimensional object (e.g., worm or membrane) whose rigidity is dominated by interfacial tension has

$$\kappa = \phi\gamma d^{4-D}$$

where ϕ is an interfacial coupling constant, γ is the interfacial tension, and d is the diameter of the hydophobic core. For a worm $D = 1$, and for a membrane $D = 2$. In a separate study of a MW series of worm-forming copolymers $\kappa \sim d^{2.8}$, as will be presented elsewhere.[7] Recently described nanofibers[22] composed of polystyrene−polyisoprene diblock copolymers in tetrahydrofuran (THF) have been reported to have l_P's ranging from ∼150 to ∼620 nm based on bulk light scattering and viscometry. An estimated core diameter of $d \approx 12$ nm from thin film characterization of the nanofibers[22] would indeed suggest a slightly lower l_P than that found here where $d \approx 14$ nm. In addition, THF (as opposed to water) in the nanofiber system is likely to give a smaller γ, which also tends to reduce l_P of the cited nanofibers.

Using $\gamma = 25$ pN/nm as a typical interfacial tension for the present block copolymer assemblies[23] and $d = 14$ nm,[4] we solve here for ϕ with $\kappa = k_BTl_P$ and obtain $\phi \approx 0.05$. This ϕ is slightly greater than that found for either lipid bilayers (∼0.03)[24] or polymer vesicle membranes (∼0.02)[1] and suggests that the worm core is effectively well coupled or interdigitated even in the absence of copolymer cross-linking.

Cross-Linking in Core-Percolated Rigidity. While an un-cross-linked worm of either OB3 or OE6 explores much of the configuration space available to it in a few seconds (Figure 2a), a fully cross-linked worm of OB3 barely flexes and instead exhibits rigid-body rotation (Figure 2b). The free radical polymerization here uses a water-soluble redox combination[25] of potassium persulfate ($K_2S_2O_8$) and sodium metabisulfate ($Na_2S_2O_5$)−ferrous sulfate ($FeSO_4{\cdot}7H_2O$) under well-stirred conditions. A very similar PEO−PBD system (EO_{37}−BD_{28}), which generates worms and vesicles coexisting in water, has instead been cross-linked by γ-irradiation with a ^{60}Co source and has also been proven stable in THF.[26] Complete cross-linking of the present system has been verified elsewhere[4] by testing the chloroform extractability of copolymer.[4] Kinks and highly contorted shapes are locked in upon cross-linking (Figure 2b). Dynamic bending modes persist nonetheless and are significantly faster after cross-linking: $\tau_{R/L} = 0.2 \pm 0.1$ s (Figure 2c).

Estimation of l_P for such rodlike objects where $l_P \gg L$ has been the subject of relatively recent study.[9,21] In the first cited reference, long microtubules ($L \sim 30$ μm) with persistence lengths known to be millimeters were analyzed by a Fourier analysis of the thermally excited bending undulations. Each normal mode has a thermal energy of ${}^1/_2k_BT$, and the sum of modes is cumulatively resisted by the strain energy to bending the rod, which is scaled by the bending rigidity κ. With the locked-in shapes here of cross-linked OB3, we subtract off the

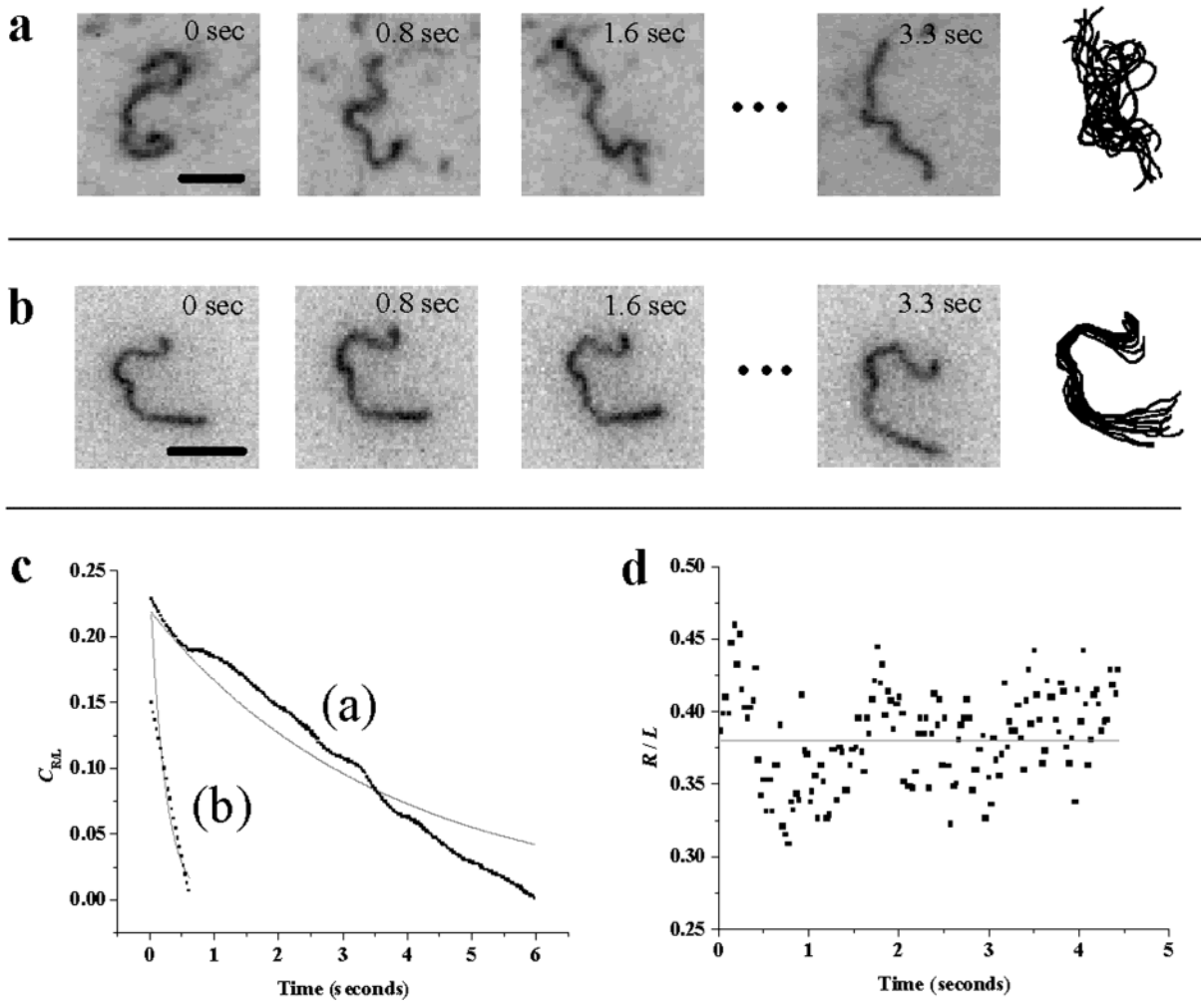

Figure 2. Snapshots (inversely intensified) and backbone traces of pristine and completely cross-linked wormlike micelles. Worms are confined between two glass coverslips spaced ~1μm apart. (a) The pristine worm explores much of the available configuration space ($l_P \approx 0.5$ μm), $\tau_{R/L} \approx 2.6$ s; 15 backbone traces are overlaid. (b) Chemically cross-linked worm shows dynamics similar to rigid body rotation ($l_P \approx 115$ μm), $\tau_{R/L} \approx 0.2$ s; 10 backbone traces are overlaid. Persistence lengths are for 3D. Scale bars are 5 μm. (c) Representative exponential fits of autocorrelation function decays in R/L vs time for pristine (a) and fully cross-linked worms (b). The difference highlights the disparate dynamics between the two systems. (d) Plot of R/L as a function of time for fully cross-linked worms, showing that the rodlike worms are ergodic objects at these time scales.

spontaneously curved average shape and perform a Fourier analysis on the first three modes as they deviate from the average shape. Surprisingly, perhaps, the system appears ergodic (Figure 2d), with each mode adequately accessed. Note also that $\tau_{R/L}$ reported above is small compared to the minimal analysis time of ~3 s. The normal-mode analysis[9] yields a 3D $\kappa = 0.46$ pN μm^2 and an $l_P = 115 \pm 30$ μm. This agrees with small-angle neutron scattering results on these cross-linked worms, despite the potential limitations of such scattering and the need to assume a model—in this case a solid beam.[27] Indeed, for a solid beam $\kappa \sim d^4$ rather than d^3 as above for pristine worms. The Young's modulus, E, of a solid worm with a cross-linked hydrophobic core can also be obtained from $l_P = EI/k_BT$, where $I = \pi(d/2)^4/4$ is the cross-sectional moment of inertia[9] and $d = 12.4$ nm is the diameter of a cross-linked worm.[4] This yields $E = 400$ MPa, which far exceeds moduli obtained with macroscopic samples of cross-linked polybutadiene (<10 MPa) and implies that the confined cross-linking here is extraordinarily efficient.

Blending of copolymers before hydration followed by cross-linking leads to worms containing both inert PEO−PEE (OE6) and cross-linked PEO−PBD (OB3). This gives l_P's that range continuously from ~0.5 to ~100 μm, which is equivalent in range to the bending rigidities of biopolymers as diverse as neurofilaments,[28] F-actin,[9] and (almost) microtubules.[9] The fluctuation dynamics of the partially cross-linked systems (as measured by the relaxation time, $\tau_{R/L}$) also show a strong dependence on the cross-linking mole fraction, X, of OB3 in OE6. For X below the percolation point X_C (≈0.15 mole fraction OB3 in OE6), $\tau_{R/L}$ is relatively constant, whereas for X above X_C, $\tau_{R/L}$ decays exponentially (Figure 3c). This decay above X_C reflects the increasing stiffness of an overdamped system, and the lack of a strong peak in $\tau_{R/L}$ near X_C[29] indicates that the viscosity of a worm's core is not a significant factor in worm dynamics. Below X_C, relaxation can thus be attributed to hydrodynamics of the embedding aqueous media.

The effective stiffness of partially cross-linked worms formed by copolymer blending is revealed in the end-to-end length-normalized fluctuations of a worm, i.e., $\langle\delta(R/L)^{-2}\rangle$ (Figure 3). By this metric, covalent cross-links begin to percolate along the hydrophobic butadiene core at the same $X_C \approx 0.15$. Below X_C, the worm is clearly a fluid, whereas above X_C, the worm is solid with a linear

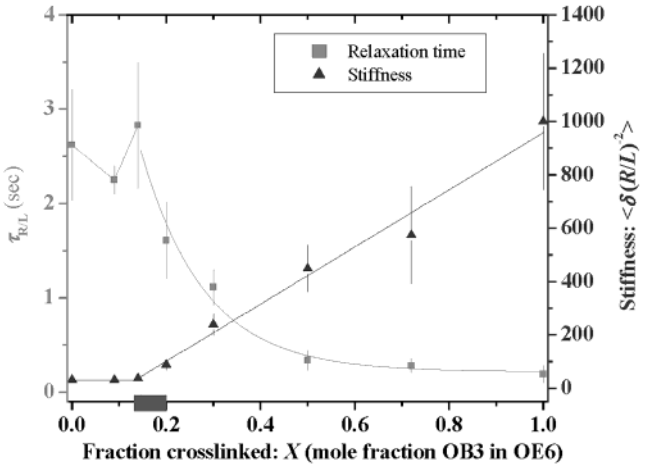

Figure 3. Worm micelle dynamics and stiffness measures as a function of cross-linking. Worms with cross-linked OB3 in OE6 (OB3 mole fraction, X) below the percolation point, $X < X_C$ ($\approx$0.15), have very similar relaxation times, $\tau_{R/L}$, for normalized end-to-end length, R/L. Worms above the percolation point have decreasing $\tau_{R/L} \sim \tau_0 \exp[-\zeta(X - X_C)]$, where τ_0 is the average relaxation time below percolation and $\zeta \approx 7$ is the damping coefficient representing the increase in internal viscosity. The effective stiffness of the partially cross-linked worms is given by the fluctuations in R/L, $\langle\delta(R/L)^2\rangle = \langle(R/L)^2\rangle - \langle R/L\rangle^2$. For $X < X_C$, worms have very similar stiffness, whereas for $X > X_C$, worm stiffness increases linearly with a slope of 11.

increase in effective stiffness. Phase separation of the two copolymers seems unlikely since the error bars are not large for $\langle\delta(R/L)^{-2}\rangle$, and no discontinuities in stiffness along single blended worms were observed.[23] The same X_C and linear increase in elasticity for $X > X_C$ have been observed in fluid-to-solid transitions of cross-linked polymer vesicle membranes[23] that are assembled from similar blends of copolymers with suitably reduced w_{EO} (i.e., $w_{EO} \sim 25-45\%$).

Flow Stretching. Theories for stretching Gaussian chains under moderate flows in various geometries[30] have already been put to the test by experiments on single DNA molecules.[31] While holding one end fixed,[31] large extensions in the direction of flow (>30% of L) have shown that the fractional extension x/L of DNA scales with νL^{ω} ($\omega = 0.54 \pm 0.05$), where ν is the mean flow velocity. This scaling is shared, in theory, by all semiflexible polymer systems (hence universal) since a modified wormlike chain model accounts for the experimental data at least for chains up to $L \approx 40$ μm.[32,33] Universality is experimentally confirmed in the initial tests here since the directional elongation of pristine worms scales as $\nu L^{0.52} \pm 0.01$ (Figure 4). Snapshots and backbone traces of un-cross-linked worms extended under various flow velocities (Figure 5a,b) also appear qualitatively consistent with theoretical "trumpet" shapes,[30] which become increasingly narrowed and stretched out under high flow (although $Re < 1$).[30]

Importantly, the worms here do not fragment under flow-imposed tensions that we estimate reach $\sim$1 μN/m. Tension on worms is calculated from a plane Poiseuille flow model with a velocity profile $v_x(y) = 3\nu[1 - (y/H)^2]$, where ν is the average flow velocity, y is the distance between coverslips, and H is the gap height. The tension is the shear stress ($\mu\ \partial v_x/\partial y$; μ is the viscosity) integrated over the contour length of each worm. While not an issue for covalent polymers such as DNA, integrity under stress is in line with the stable distributions of worm lengths of Figure 1c and indicates that this is more of a stable aggregate than a living polymer.

Consistent with cross-link-enhanced stability but contrasting with the trumpet-shaped envelopes, the backbones of totally cross-linked worms are largely unaffected by flow (Figure 4c). Spontaneous curvature of these cross-linked micelles is truly locked in while the worm thermally fluctuates with or without externally imposed forces. If minimization of kinks is desired for a particular application, cross-linking can be done while either stretching worms under shear as here or lyotropically straightening for a particular application the worms in dense solutions of mesogens of the same or dissimilar type (e.g., rodlike phages or viruses).[34]

Pristine worms, and polymeric objects in general, also tend to stretch out when flowing through a confining structure such as a pore or a microcapillary. Aspiration of a pristine worm into a micropipet shows initial

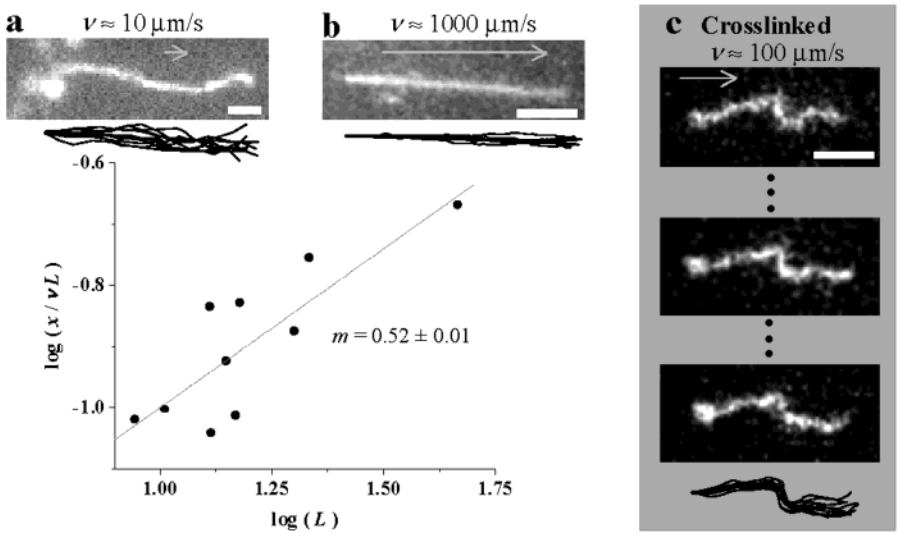

Figure 4. Worms in flow. (a, b) Flow-induced extension of un-cross-linked worms where one end is fixed to a glass coverslip. Snapshots at low and high flow velocities, respectively, show trumpet shapes when backbones are overlaid. The mean flow velocity, ν, is estimated from smaller micelles flowing past, and the plot shows that normalized worm extension, x/L, scales as $\nu L^{0.52} \pm 0.01$. (c) Snapshots of an attached, fully cross-linked worm under flow. Note that the kink along the backbone is minimally perturbed by the flow. Scale bars are 5 μm.

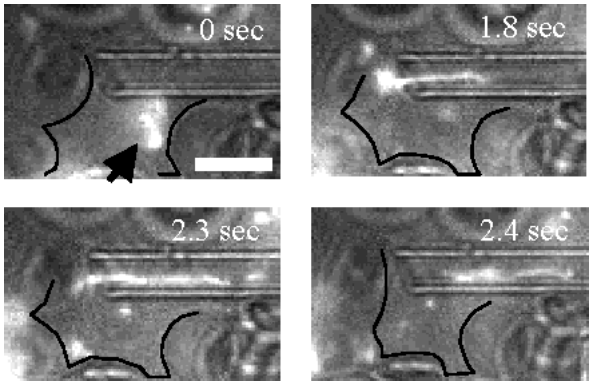

Figure 5. Worm extension in capillary flow. Snapshots of a pristine worm drawn into a 4 μm diameter glass capillary from a chamber filled with blood cells ($v \approx 35$ μm/s). The black lines mark the edges of several cells around the worm micelles. Scale bar is 5 μm.

diffusion in bulk among cells followed by convective alignment into the micropipet (Figure 5). The entry transition at $t = 1.8$ s shows the bright section of the worm outside, still diffusing in bulk, while the last two snapshots show the worm fully extending and traveling down the pipet. This behavior is the inverse of that in Figure 1b and shows that pristine worms are equally adept at stealthily traveling in complex fluid flows as they are at diffusively expanding into a stagnant zone or cavity.

One final important aspect of the experiments illustrated in Figures 1b and 5 is the evident stability of the worms among cells and in blood plasma composed of thousands of proteins, fatty acids, and other surface active agents. This inertness undoubtedly stems from the stealthiness imparted by the PEO which is also absolutely central to worm formation and not merely an additive as with PEG lipid in so-called "stealthy" liposomes.

Conclusions

Worm micelles assembled from PEO-based nonionic copolymers prove extremely stable in aqueous media, and the dynamics of the worms can be directly visualized with fluorescence microscopy techniques. By blending and polymerizing inert (OE6) and cross-linkable (OB3) copolymers, we form micelles up to tens of microns long (or longer) with persistence lengths from 500 nm to 100 μm. The persistence length of the pristine worms is just large enough for the backbone to be clearly visualized when the worm is confined in a gap or a microcapillary. In flow, pristine worms orient and stretch with DNA-like scaling. The combination of their stability, hydrophobic loading capacity, and PEO-imparted stealthiness suggests such worm micelles to be suitable for flow-intensive delivery applications such as phage-mimetic drug carriers and micropore delivery.

Acknowledgment. The authors thank J. Crocker and C. Storm for valuable discussions. This work was supported by NSF-MRSEC's at Penn and University of Minnesota.

References and Notes

(1) Discher, B. M.; Won, Y. Y.; Ege, D. S.; Lee, J. C. M.; Bates, F. S.; Discher, D. E.; Hammer, D. A. *Science* **1999**, *284*, 1143.
(2) Hajduk, D. A.; Kossuth, M. B.; Hillmyer, M. A.; Bates, F. S. *J. Phys. Chem. B* **1998**, *102*, 4269.
(3) Zhang, L. F.; Eisenberg, A. *Science* **1995**, *268*, 1728.
(4) Won, Y. Y.; Davis, H. T.; Bates, F. S. *Science* **1999**, *283*, 960.
(5) Israelachvili, J. In *Intermolecular & Surface Forces*; Academic Press: London, 1992.
(6) Won, Y. Y.; Paso, K.; Davis, H. T.; Bates, F. S. *J. Phys. Chem. B* **2001**, *105*, 8302.
(7) Dalhaimer, P.; Bermudez, H.; Discher, D. E., submitted for publication.
(8) Maier, B.; Radler, J. O. *Phys. Rev. Lett.* **1999**, *82*, 1911.
(9) Gittes, F.; Mickey, B.; Nettleton, J.; Howard, J. *J. Cell Biol.* **1993**, *120*, 923.
(10) Ott, A.; Magnasco, M.; Simon, A.; Libchaber, A. *Phys. Rev. E* **1993**, *48*, 1642.
(11) Tang, J. X.; Janmey, P. A. *J. Biol. Chem.* **1996**, *271*, 8556.
(12) Janmey, P. A.; Hvidt, S.; Oster, G. F.; Lamb, J.; Stossel, T. P.; Hartwig, J. H. *Nature (London)* **1990**, *347*, 95.
(13) Xu, J.; Schwartz, W. H.; Kas, J. A.; Stossel, T. P.; Janmey, P. A.; Pollard, T. D. *Biophys. J.* **1998**, *74*, 2731.
(14) Poirier, M. G.; Marko, J. F. *Phys. Rev. Lett.* **2002**, 228103.
(15) Walker, L. M. *Curr. Opin. Colloid Interface Sci.* **2001**, *6*, 451.
(16) Mackintosh, F. C.; Kas, J.; Janmey, P. A. *Phys. Rev. Lett.* **1995**, *75*, 4425.
(17) Hillmyer, M. A.; Bates, F. S. *Macromolecules* **1996**, *29*, 6994.
(18) Menger, F. M.; Angelova, M. I. *Acc. Chem. Res.* **1998**, *31*, 798.
(19) Flory, P. J. In *Statistical Mechanics of Chained Molecules*; Wiley: New York, 1969.
(20) Grosberg, A. Y.; Khokhlov, A. R. *Statistical Physics of Macromolecules*; AIP Press: New York, 1994.
(21) Wilhelm, J.; Frey, E. *Phys. Rev. Lett.* **1996**, *77*, 2581.
(22) Liu, G.; Yan, X.; Duncan, S. *Macromolecules* **2003**, *36*, 2049.
(23) Discher, B. M.; Bermudez, H.; Hammer, D. A.; Discher, D. E.; Won, Y. Y.; Bates, F. S. *J. Phys. Chem. B* **2002**, *106*, 2848.
(24) Goetz, R.; Gompper, G.; Lipowsky, R. *Phys. Rev. Lett.* **1999**, *82*, 221.
(25) Odian, G. *Principles of Polymerization*, 3rd ed.; Wiley: New York, 1991.
(26) Maskos, M.; Harris, J. R. *Macromol. Rapid Commun.* **2001**, *22*, 271.
(27) Won, Y. Y.; Davis, H. T.; Bates, F. S.; Agamalian, M.; Wignall, G. D. *J. Phys. Chem. B* **2000**, *104*, 7134.
(28) Janmey, P. A.; Euteneuer, U.; Traub, P.; Schliwa, M. *J. Cell Biol.* **1991**, *113*, 155.
(29) Muhammad, S. *Applications of Percolation Theory*; Taylor & Francis Inc.: London, 1994.
(30) Brochard-Wyart, F. *Europhys. Lett.* **1993**, *23*, 105.
(31) Perkins, T.; Smith, D. E.; Larson, R. G.; Chu, S. *Science* **1995**, *268*, 83.
(32) Marko, J. F.; Siggia, E. D. *Macromolecules* **1997**, *28*, 8759.
(33) Larson, R. G.; Perkins, T.; Smith, D. E.; Chu, S. *Phys. Rev. E* **1997**, *55*, 1794.
(34) Dogic, Z.; et al. Manuscript in preparation.

MA034120D